Supplementary Information for

Proteome-Wide Effects of Naphthalene-Derived Secondary Organic Aerosol in BEAS-2B Cells Are Caused by Short-Lived Unsaturated Carbonyls

Jiajun Han[a, 1], Shunyao Wang [b, 1], Kirsten Yeung[a], Diwen Yang[a], Wen Gu[c], Zhiyuan Ma[d], Jianxian Sun[a], Xiaomin Wang[e], Chung-Wai Chow[e], Arthur W. H. Chan [a,b,f,2], Hui Peng [a,f,2]

Hui Peng,

Email: hui.peng@utoronto.ca

Arthur W. H. Chan,

Email: arthurwh.chan@utoronto.ca

This PDF file includes:

Supplementary text

Figures S1 to S13

SI References

www.pnas.org/cgi/doi/10.1073/pnas.2001378117

Supplementary Information Text

Materials and Methods

Chemicals and Reagents. Naphthalene, methanol, dimethyl sulfoxide (DMSO), triethyl ammonium bicarbonate buffer (TEAB), tris(2-carboxyethyl) phosphine hydrochloride (TCEP), iodoacetamide, cOmplete Mini EDTA-free protease inhibitor cocktail tablets, Dulbecco's Modified Eagle's Medium – high glucose (DMEM) and dithiothreitol (DTT) were purchased from Sigma-Aldrich (St. Louis, MO, USA). HEPES and Phosphate-Buffered Saline tablets were obtained from the BioShop Canada Inc. (Burlington, ON, Canada). BEAS-2B, a human bronchial epithelial cell line, was provided by Dr. C. Harris (National Cancer Institute, National Institutes of Health, Bethesda, MD). Bronchial epithelial cell growth basal medium (BEBM) supplemented with bronchial epithelial cell growth medium (BEGM) SingleQuots (Lonza, Basel, Switzerland) was used as growth media for the BEAS-2B cell line. Antibiotic antimycotic solution, fetal bovine serum (FBS), G418, ultrapure water and acetonitrile (HPLC grade) were obtained from Fisher Scientific (Ottawa, ON, CA). Formic acid (mass spectrometry grade) was purchased from EMO Millipore (St. Louis, MO, USA). Trypsin Gold (Mass Spectrometry Grade) from Promega (Madison, WI, USA) was used for protein digestion. Toptip (TT2C18) from Glygen Corp. (Columbia, MD, USA) was chosen for proteome sample desalting. All other chemicals were the highest grade available.

NSOA Collection and Extraction. A custom-built scanning mobility particle sizer made with a differential mobility analyzer (DMA, Model 3081, TSI, Shoreview, MN, USA) and a condensation particle counter (CPC, Model 3772, TSI, Shoreview, MN, USA) was used to monitor the particle size distribution and volume concentration exiting the flow tube. Custom code written in Igor Pro (Wavemetrics, Portland, OR, USA) was used for particle data inversion. The mass concentration of SOA was derived by assuming a particle density of 1.5 g cm^{-3}. SOA yields are expressed as the mass fraction of SOA formed relative to the mass of naphthalene reacted.

NSOA was collected on prebaked (500 °C, 12 h) quartz fiber filters (47 mm, Pall, USA) with the total mass calculated by integrating mass concentration, flow rate and collection time. Filter punches were taken directly from the NSOA filter immediately after synthesis for GC/MS analysis. For further chemical

characterization and *in vitro* studies, the remaining NSOA filters were extracted using 5 mL methanol with 3-minute ultrasonication after flow tube collection with insoluble materials filtered out by PTFE syringe filters (0.22 μm, Fisherbrand™).

GC/MS Analysis. NSOA quartz filter samples were directly analyzed using thermal desorption (TDS 3, Gerstel, USA)-gas chromatography-mass spectrometry (TD-GC/MS; 7890B, 5977A, Agilent, USA). 4 mm diameter filter punches were inserted into glass tubes (6 mm OD x 178 mm length, Gerstel, USA) and placed in the TDS for thermal desorption. To track the recovery efficiency of identified NSOA compounds, each sample was spiked with a known amount of deuterated anthraquinone (98 atom % D, Sigma Aldrich) prior to thermal desorption in the TDS as an internal standard. The temperature ramping program for thermal desorption was from 40 °C initial temperature followed by a ramp program of 60 °C min^{-1} to 320 °C and held for 5 minutes at 320 °C. Once the sample punches were desorbed in the TDS, the desorbed organics were transferred to the cooling injection system (CIS4, Gerstel, USA) via a transfer line maintained at 300 °C during the run. The CIS4 was embedded with quartz wool filled quartz liner maintained at 20 °C during thermal desorption to preconcentrate the desorbed analytes. Once thermal desorption was complete, the CIS was heated from 20 °C to 320 °C at 12 °C s^{-1}, and held for an additional 10 minutes at 320 °C. The GC column was a non-polar Rxi-5ms column (Restek, USA) with dimensions of 30 m × 250 μm × 0.25 μm and was heated from 50 °C to 300 °C at a ramp of 8 °C min^{-1} and held for an additional time of 4 minutes at 300 °C for analysis. All samples were analyzed under electron impact at 70 eV using a standard tungsten filament with a source temperature at 230 °C. The MS was operated at 3.1 scans s^{-1} with an acquisition range from mass-to-charge (*m/z*) ratio between 35 and 500. Identification was based on both mass spectral library match and NIST retention indices. Relative abundance of each assigned NSOA composition was calculated by peak area integration in MassHunter Workstation (Agilent, v B.06.00), and further normalized to the peak area of deuterated anthraquinone in each run.

LC-Orbitrap Analysis. For chemical profiling of NSOA, 3 μL of each sample was loaded onto a Accucore Vanquish C18 UHPLC Column (80 Å; 1.5 μm; 2.1 mm × 50 mm, Thermo Scientific, Waltham, Massachusetts, United States) driven by a Vanquish ultra-high-performance liquid chromatography (UHPLC) system (Thermo Fisher Scientific) tandem Q Exactive mass spectrometer (Thermo Fisher

Scientific). The mobile phases used were as follows: (A) HPLC grade water (0.1% formic acid); (B) acetonitrile (0.1% formic acid). 3 minutes after injection, B was increased from 2% to 30% then increased to 100% in next 3 minutes and kept static for 2.8 minutes. In rapid succession, B was returned to 2% within 0.2 minutes and kept 1 minute for column equilibration. The temperature of sampler and column oven were maintained at 4 °C and 40 °C respectively. The MS data was acquired using a full MS scan (100 to 1000 m/z) at 70,000 resolution (at *m/z* 200) with a maximum of 3×10^6 ions collected within 100 ms. The MS/MS data was recorded by an All Ion Fragmentation (AIF) workflow with 70,000 resolution and a maximum of 3×10^6 ions collected within 100 ms. Both negative ion and positive ion mode were operated with a 10-minute method. The general mass spectrometry settings for electrospray ionization (ESI) mode are shown as follows: spray voltage, 2.7 kV; capillary temperature, 300 °C; sheath gas, 30 L/h; aux gas, 6 L/h; and aux gas heater temperature, 325 °C.

IMS-TOF-MS Analysis. Extracted NSOA was reconstituted to a concentration of 1 mg mL^{-1} by N_2 (5.0 L min^{-1}) under the N-EVAP blow-off system (Organomation, USA). The reconstituted solution was delivered by a syringe pump (KDS Legato100) along with the sample transfer line (360 µm OD, 50 µm ID, 50 cm length, New Objective, USA) before reaching the ESI source. The ESI source is made of an uncoated SilicaTip emitter (New Objective, US), where charged NSOA solution can be emitted as a beam of Tyler Cone droplets and sent to the desolvation region by N_2 (1 L min^{-1}). In the desolvation region, analytes get charged as the solvent gradually being evaporated until single ions formed via fission cycles. The ions were further sent to the IMS drift tube through a Bradbury-Nielsen gate operated under the Hadamard transform mode (1). The ESI source and the IMS gate temperature were both set to 60 °C with operation pressure set to 1000 mbar. After entering the ion gate, ion mobility of the analytes can be measured inside the drift tube by colliding with the N_2 buffer gas (1.2 L min^{-1}). The averaged velocity of an ion (v_i, m s^{-1}) moving inside the drift cell is related with the characteristic mobility constant (K, m^2 V^{-1} s^{-1}) and the electrical field intensity (E, V m^{-1}):

$$v_i = KE \quad (1)$$

IMS measured drift time t_i (s) of an ion can be derived from:

$$t_i = \frac{L^2}{VK} \quad (2)$$

L is the length (m) of the drift tube, and V is the applied electric filed potential (V) of the drift tube. The measured drift time is related with temperature and pressure while the reduced mobility (K_0, $m^2\ V^{-1}\ s^{-1}$) is an intrinsic parameter of each specific molecular ion being measured:

$$K_0 = \frac{L^2}{V t_i} \frac{P}{1013.25} \frac{273.15}{T} \quad (3)$$

where P is the experimental pressure (mbar), and T is the experimental temperature (K) (2).

The K_0 value for a specific ion can still be slightly varied from various experiments because of the uncertainty of the drift tube pressure and temperature that can impact the drift time measurement accuracy while the molecular collision cross section (CCS, Ω) can be derived from K_0 using the Mason–Schamp equation when IMS is calibrated and well-operated (3-5).

$$\Omega = \frac{3ze}{16N_0} \left(\frac{2\pi}{k\mu T_0}\right)^{1/2} \frac{1}{K_0} \left[1 + \left(\frac{v_d}{v_T}\right)^2 \left(\frac{\beta_{MT}}{\alpha_{MT}}\right)^2\right]^{-1/2} \quad (4)$$

in which z is the charge number, q is the elementary charge (1.60×10^{-19} C), N_0 is the neutral gas number density, k is the Boltzmann constant ($1.38 \times 10^{-23}\ m^2\ kg\ s^{-2}\ K^{-1}$), μ is the reduced mass of the ion buffer gas pair, T_0 is the standard temperature, v_d is the drift velocity, v_T is the thermal velocity, β_{MT} is the correction factor for momentum transfer, and α_{MT} is the correction factor for collision frequency, which can be calculated as:

$$\alpha_{MT} = \frac{2}{3}\left[1 + \hat{m}\hat{C} + \hat{M}\hat{H}\right] \quad (5)$$

$$\beta_{MT} = \left[\frac{2}{\hat{m}(1+\hat{m})}\right]^{1/2} \quad (6)$$

where $\hat{m}$ and $\hat{M}$ are the ion and neutral gas mass fraction in the collision pair. $\hat{C}$ and $\hat{H}$ are the fraction of collisions that cool and heat the ion. After the millisecond-timescale separation in the IMS drift tube, the ion will be carried to the second spectrometer by N_2 buffer gas and detected by TOF-MS with microsecond timescale. The mass resolution of the TOF-MS is within 3500–4000 FWHM at m/z 250 (6). IMS data recording was performed by “Acquility” (v. 2.1.2), with data processing completed by “Tofware” (v. 2.5.7), built in Igor Pro (WaveMetrics, OR, USA).

In this study, trajectory model (TM) predicted CCS (7, 8) was used to compare with the IMS measured CCS to further propose the molecular structure of major NSOA compounds. The potential (short-range van der Waals interactions and the long-range ion-induced dipole interactions) employed in the TM calculation for a given drift gas can be expressed as:

$$\Phi(\theta, \Phi, \gamma, b, r) = 4\epsilon \sum_i^n [(\frac{\sigma}{r_i})^{12} - (\frac{\sigma}{r_i})^6] - \frac{\alpha_p}{2}(\frac{ze}{n})^2[(\sum_i^n \frac{x_i}{r_i^3})^2 + (\sum_i^n \frac{y}{r_i^3})^2 + (\sum_i^n \frac{z_i}{r_i^3})^2] \quad (7)$$

where θ, Φ, γ are the three angles that describes the geometry of the ion collision pair, b is the impact factor, r is the distance between the mass center of the ion and the neutral molecule, ϵ is the depth of the potential well, σ is the value of distance (r) at the minimum (zero) potential, and αp is the neutral polarizability (1.710×10^{-24} cm^3 for N_2) (9), x_i, y_i, z_i and r_i are the relative coordination of the ion to the neutral gas molecule.

A schematic of the CCS comparison method can be found in Fig. S3. First, molecular formulas were assigned for the most abundant peaks detected by the HR-HPLC-MS/MS. Structures for a specific molecular formula assigned were further given by the NIST Chemistry Webbook (https://webbook.nist.gov/chemistry/). As a following step, possible structures in NSOA were selected out. The selected NSOA structures were further constructed in Avogadro (v1.0.1) (10), with atomic and charge information exported by the built in Python terminal after ionic geometry optimization (11). The exported information was further input to the MOBCAL programme (https://www.indiana.edu/~nano/%20software/) and then calculated the theoretical CCS using the trajectory method (7, 12, 13). The predicted TM CCS from different isomeric structures were collected and compared to the IMS measured CCS (1). The molecular structure with predicted CCS value that is the closest to the empirical value was eventually assigned as the most possible structure for the MS measured NSOA signal. Measured CCS and theoretically predicted CCS for the final assigned structures were plotted against each other in Fig. S4.

ROS Measurement by EPR. Electron paramagnetic resonance (EPR) was used to directly quantify the reactive oxygen species (ROS) in NSOA samples. A continuous-wave electron paramagnetic resonance (CW EPR) spectroscopy (X-band, ECS-EMXplus, Bruker, Germany) combined with a spin-trap technique (TEMPONE-H, Enzo Life Sciences GmbH) (14) was applied in ROS measurements. For sample preparation, extracted NSOA was gently dried under N_2 (5.0 L min^{-1}) and immediately reconstituted to 10 mg mL^{-1} in an aqueous solution of the spin probe (20mM). A final volume of 10-20 µL of the sample solution was prepared for EPR analysis with a highly sensitive cavity (ER 4123D). During the analysis, the receiver gain was set to 30 dB. The microwave power was 0.214 mW. The modulation frequency was set to 100 kHz with a modulation amplitude of 1. The magnetic field sweep width was 204.8 G and the time constant was 0.01 ms.

Spin quantification (ROS abundance) was achieved using the built-in spin counting method of the Bruker Xenon software (15). The number of spins in the sample can be derived by performing double integration of the peak intensity, which involves the following equation:

$$DI = c\,[G_R\ C_t\ n]\,[\frac{\sqrt{P}\ B_m\ Q\ n_B\ S(S+1)n_S}{f(B_1,B_m)}] \quad (8)$$

in which c is the constant determined by a standard sample with known number of spins, G_R is the value of receiver gain, C_t is the conversion time, n is the number of scans, P is the microwave power, B_m is the modulation amplitude, Q is the quality factor of resonator, n_B is the Boltzmann factor for temperature dependence, S is the total electron spin, n_s is number of spins, $f(B_1, B_m)$ is the sample experienced spatial distribution of the microwave field and the modulation field (16).

Cell Viability Assay of BEAS-2B. We are interested in sub-cytotoxicity effects, thus the MTT Cell Viability Assay Kit (Biotium, Hayward, CA) was used to assess BEAS-2B cell viability according to the manufacturer's protocol. Briefly, 5×10^4 cells were seeded into each well in a 96 well plate and incubated at 37 °C for 24 hr to reach approximately 80% confluence. Subsequently, the growth medium was replaced by exposure medium (no growth factor) and NSOA (vehicle solvent < 0.1%) was introduced to each well. After a 24-hour exposure at 37 °C in a CO_2 incubator, 10 µL of 12 mM MTT were added into each well and a 4-hour incubation at 37 °C was performed. The generated formazan product was dissolved and photometrically quantified at 570 nm using a microplate reader (PHERAstar FSX, BMG Labtech). The result is presented as percent relative to vehicle control group, no significant cytotoxicity (viability > 80%) was observed in 50 µM or 100 µM NSOAs exposure.

Sample Preparation for Proteome Analysis. A freeze-thaw cycle was performed 3 times between the -80 °C freezer and 37 °C water bath to open the cell walls. Then the cells were lysed using the Ultrasonic Sonifier SFX250 Cell Disruptor (BRANSON). After centrifugation at 15,000 × g for 15 minutes at 4 °C, the supernatant was transferred to new tubes where the lysate's total protein concentration was determined by the Bradford assay with bovine serum albumin (BSA) as a standard. In order to remove interfering compounds, especially any remaining protease inhibitor, aliquots of 20 µg protein of each sample were precipitated with 4 times its volume of acetone at -20 °C overnight. The supernatant was decanted after centrifugation at 15,000 × g for 15 minutes at 4 °C. The pellet was then air dried and resuspended with 100 µL of 100 mM TEAB. A 60-minute incubation of 2mM TCEP at ambient temperature was used to

reduce any disulfide bonds within the proteins. Alkylation occurred over an incubation of 30 minutes at room temperature in the dark with iodoacetamide at a final concentration of 4 mM. Proteins were further digested by trypsin at an enzyme-to-substrate ratio of 1:40 for 16 h at 37 °C and digestion was quenched by adding formic acid to a final concentration of 1%.

Stable isotope dimethyl labeling method as described previously was performed for protein quantification (17). In this work, digested peptides were isotope labeled parallelly to 3 different mass shifts respectively. Then 3 differentially labeled samples were pooled together and desalted by C18 TopTip (Glygen Columbia, MD) according to the manufacturer's instruction. Eluents were vacuum dried and reconstituted in 120 µL HPLC water with 0.1% formic acid (FA) for mass spectrometry analysis.

Proteome Analysis by Nano-LC Orbitrap. Two mobile phases were operated at a 300 nL/min flow rate: (A) 95% acetonitrile/ 5% H_2O/ 0.1% formic acid (v/v/v) (B) 5% acetonitrile/ 95% H_2O/ 0.1% formic acid (v/v/v). Initially, B was increased from 5% to 26% in 151 mins; then to 100% in the subsequent 15 mins; and kept static for 14 mins, thus the total method duration was 180 mins. The positively charged ions underwent a 300-1400 m/z full scan with 60,000 resolution, 45 ms maximum injection time (IT), and 3×10^6 automatic gain control (AGC) target. The secondary mass spectrometry data was acquired in data-dependent single ion monitor mode (dd-SIM) with 15,000 resolution, 20 ms maximum IT, 1.4 isolation window, 1×10^5 AGC target, 28 NCE, and 20 s dynamic exclusion.

Nrf2 Reporter Cell Line Exposed to NSOA. In present study, a MCF7 Cell Line which has been stably transfected with pTA-NRF2-luciferasereporter vector (Signosis) was utilized to measure NRF2 activity triggered by NSOAs. Prior to performing the Nrf2 assay, the MTT assay was conducted as aforementioned and no cytotoxicity was observed. Nrf2 assay was conducted as previously described (18), 5×10^4 Nrf2 reporter cells in 100 µL of DMEM growth medium supplemented with FBS were seeded into each well of a 96 - well flat bottom microplate and cultured for 24 hours in a humidified incubator at 37 °C with 5% CO_2. Following which, the growth median was discarded, and NSOAs which were produced in various oxidative conditions were introduced to reporter cells with 100 µL of exposure medium without FBS (n = 4). The control was dosed with same amount of vehicle solvent (0.1% DMSO, v/v). The exposure medium was removed by aspiration after a 24 h incubation and the cells were washed twice with 150 µL cold phosphate buffered saline (PBS). Then, the reporter cells were incubated with 75

ul Ca/Mg DPBs buffer and 75 ul of luciferase substrate (SteadylitePlus Kit, PerkinElmer, MA) for 30 - 45 minutes in dark at ambient temperature. Luminescence intensity was analyzed by a luminometer (PHERAstar FSX, BMG Labtech). Nrf2 activity was reported in fold changes of the luminescence intensity relative to the vehicle control group.

Chemical Probe Assay and In-Gel Fluorescence Imaging. A probe based chemical proteomics method was used to investigate the alkylation of cellular proteome by NSOA on the proteome-wide level (Fig. S10A). Firstly, NSOA was generated from 2-ethynyl-naphthalene under the same photooxidation conditions as the naphthalene experiments as described previously, producing ethynyl-NSOA which acted as chemical probes. BEAS-2B cells were then exposed to the ethynyl-NSOA for 1 h and the cells were collected with 1 mL cold PBS on ice. After centrifugation at 3, 000 × g for 5 minutes, the supernatant was discarded, and the cell pellet was stored at - 80 °C for future experiments. Ethynyl-NSOA exposed BEAS-2B cell lysate was extracted with 300 μL of lysis buffer (500 mM NaCl, 20 mM HEPES, 0.1% NP40, protease inhibitor cocktail, pH = 7.4) via sonication on ice. Total protein concentration was determined by the Bradford assay with bovine serum albumin (BSA) as a standard. 50 μL of protein (1mg/mL) from each treatment was aliquoted and incubated with 1 mM $CuSO_4$, 1 mM TCEP, 0.1 mM THPTA and 0.05 mM Azide-fluor 488 for 1 h at room temperature with shaking. The resultant Click-reactions, joining the Azide-fluor 488 to the ethynyl-NSOA, were quenched using 200 μL cold acetone and incubated at -20 °C overnight. Then, the precipitated protein was centrifuged at 14,000 × g for 15 minutes at 4 °C, the acetone was discarded, and the protein pellets were rinsed twice with 200 μL cold acetone. The protein pellet was resuspended with 30 μL of SDS-PAGE loading buffer (50 mM Tris·HCl, 2% SDS, 6% Glycerol, 0.01% Bromophenol Blue, pH 6.8) and 10 μL of each sample was analyzed by 15% SDS-PAGE and imaged via a fluorescent biomolecular imager (Typhoon FLA 9500).

Using a similar protocol (Fig. S11A), a competition assay between ethynyl-NSOA and 1,4-naphthoquinone was conducted. 50 μg BEAS-2B cell lysate was pre-incubated with 10, 100, or 1000 μM 1,4- naphthoquinone respectively for 1h, then 500 μM ethynyl-NSOA was subsequently added and incubated for 1h. Following the aforementioned click chemistry protocol, the resultant SDS-PAGE gel was imaged by the biomolecular imager. A control treatment without 1,4- naphthoquinone was also conducted in parallel.

Nontarget Data Analysis. Nontarget data analysis was accomplished with an in-house R program. Raw mass spectrometry files were converted to mzXML format. The peaks were detected with the XCMS package at a mass tolerance of 2.5 ppm. The peak features were matched across samples with a mass tolerance of 2.5 ppm and retention time window of 20 seconds, after retention time adjustment. Isotopic peaks and adducts were excluded by matching chromatographic peaks and theoretical mass difference. The final differentiated peak list from the output of the R program was manually checked using MS^1 mass and retention time. Elemental compositions of features were calculated within a mass tolerance of 3 ppm. Chemical formulas for NSOA chemicals were set to contain up to 100 C, 200 H, 5 N, and 30 O per molecule. Chemical formulas for NSOA chemicals were set to contain up to 100 C, 200 H, 1-5 N, 30 O, and 1-2 S per molecule.

Statistical Analysis. Proteins found with over 50% invalid values were omitted from further statistical analyses. Pearson correlation between replicates was used to evaluate the reproducibility of detection method. A 1.5-fold change (FC) and p-value of < 0.05 were used as thresholds to ascertain significantly changed proteins as previous study (19). ANOVA coupled with the Turkey post hoc test was performed for multiple comparisons to calculate significant differences between treatments. To visualize up and down regulated proteins, scatter plots and box plots were made by the R package “ggplot2”. “UpSetR” package was formatted to generate UpSet diagrams for the visualization of overlapped and unique proteins. Pathway enrichment and function annotation was parsed with ClueGo (v2.5.1), a plugin of Cytoscape (v3.6.1). The latest database of Homo sapiens, including KEGG, REACTOME (pathways and reactions) and GO (Biological Process and Molecular Function) were synchronized. In this study, the GO Tree Interval was set as 3 min-8 max levels. Kappa Score = 0.4 and a two-sided hypergeometric test coupled with Benjamini-Hochberg P-value correction was used as the criteria for enrichment. GO term fusion was applied as well. For all tests, $p < 0.05$ was taken to be statistically significant.

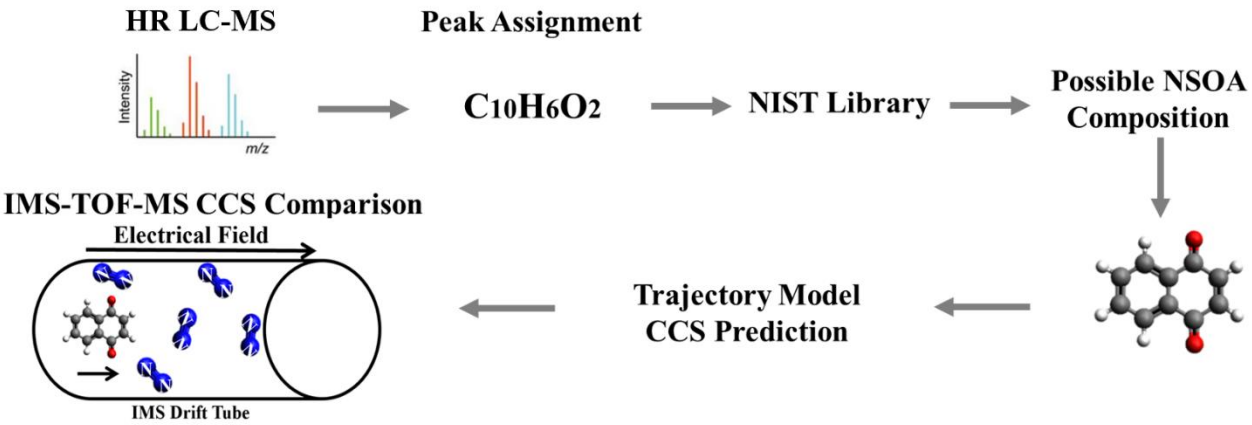

Fig. S1. Schematic of NSOA molecular structure assignment based on the mass spectrometry measurements.

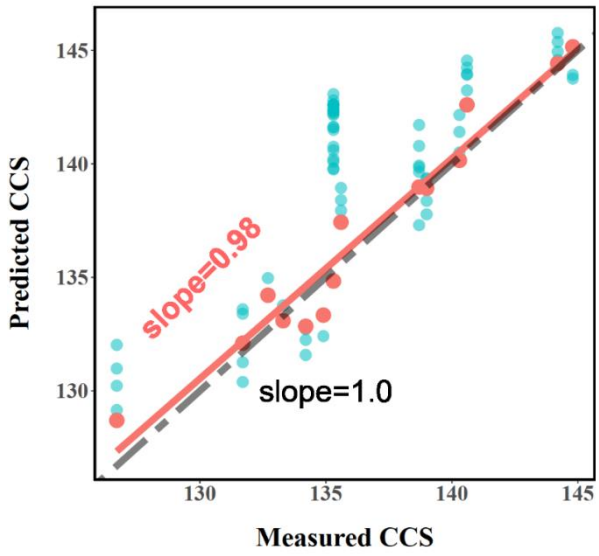

Fig. S2. Predicted CCS versus IMS measured CCS. For each compound, the molecular structure with a predicted CCS that is the closest to the measured CCS was chosen to represent the most possible molecular structure measured by LC-HRMS.

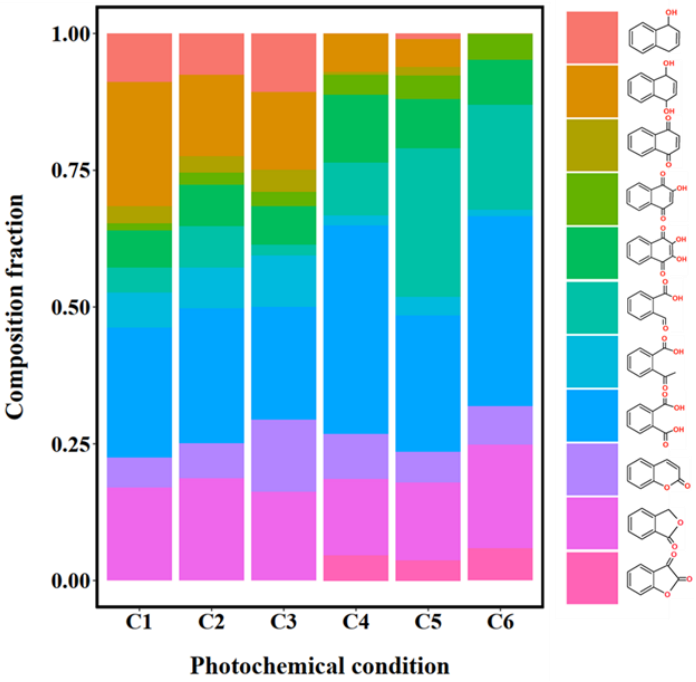

Fig. S3. Results from GC/MS analysis indicate a decreasing trend of carbonyls in NSOA from 6 different oxidation conditions, which is consistent with the cluster evolution trend illustrated in Fig. 1C determined by LC-HRMS.

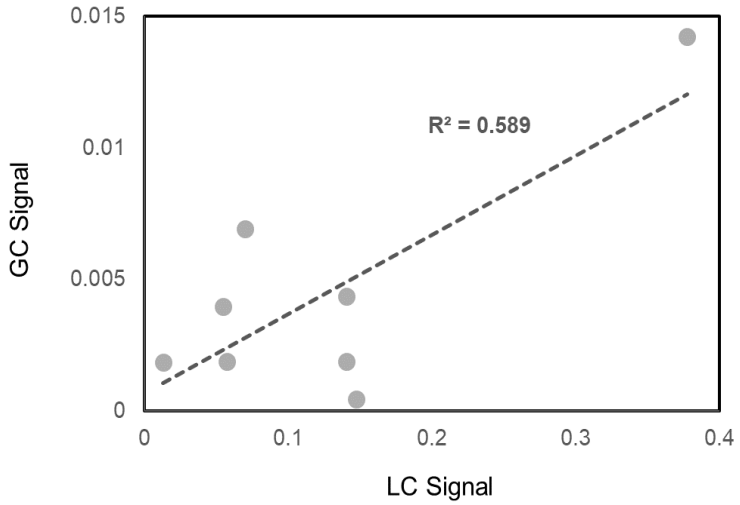

Fig. S4. Comparison of the normalized signal intensity for compounds in C1 NSOA measured from GC/MS and LC/MS.

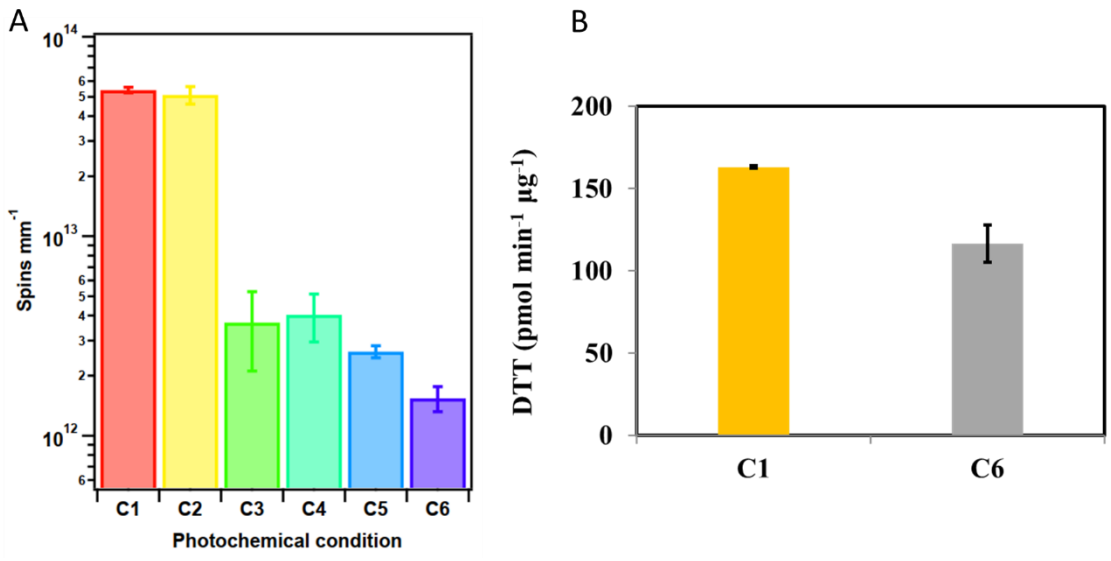

Fig. S5. EPR results indicate decreased abundance of reactive oxygen species presented in NSOA from 6 different photooxidation conditions (A). Decreased OP indicated by the DTT assay for NSOA collected from C6 compared to that of C1 (B).

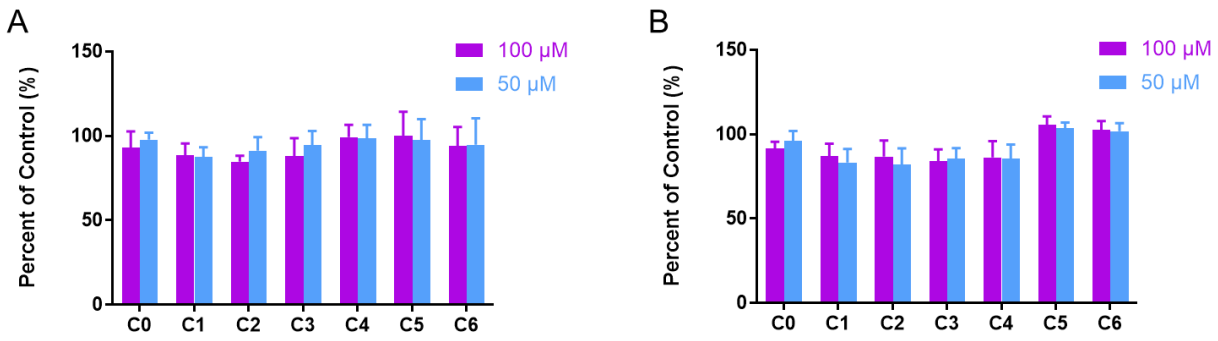

Fig. S6. Cell viability was measured by the MTT assay and results are presented as percent relative to vehicle control group. MCF7 cell line (A) and BEAS-2B cell line (B) were exposed to NSOA from 6 photooxidation conditions with two concentrations (50 µM and 100 µM). No significant cytotoxicity was observed after exposure to NSOAs at 100 µM.

Fig. S7. Effects of NSOAs on proteomic profile of BEAS-2B cell line. Heatmap presents the regulated proteins identified by proteomic assay. Values were presented as log_2 transformed fold change compared with control group. Color scale of legend ranges from blue (strongly downregulated) to red (strongly upregulated).

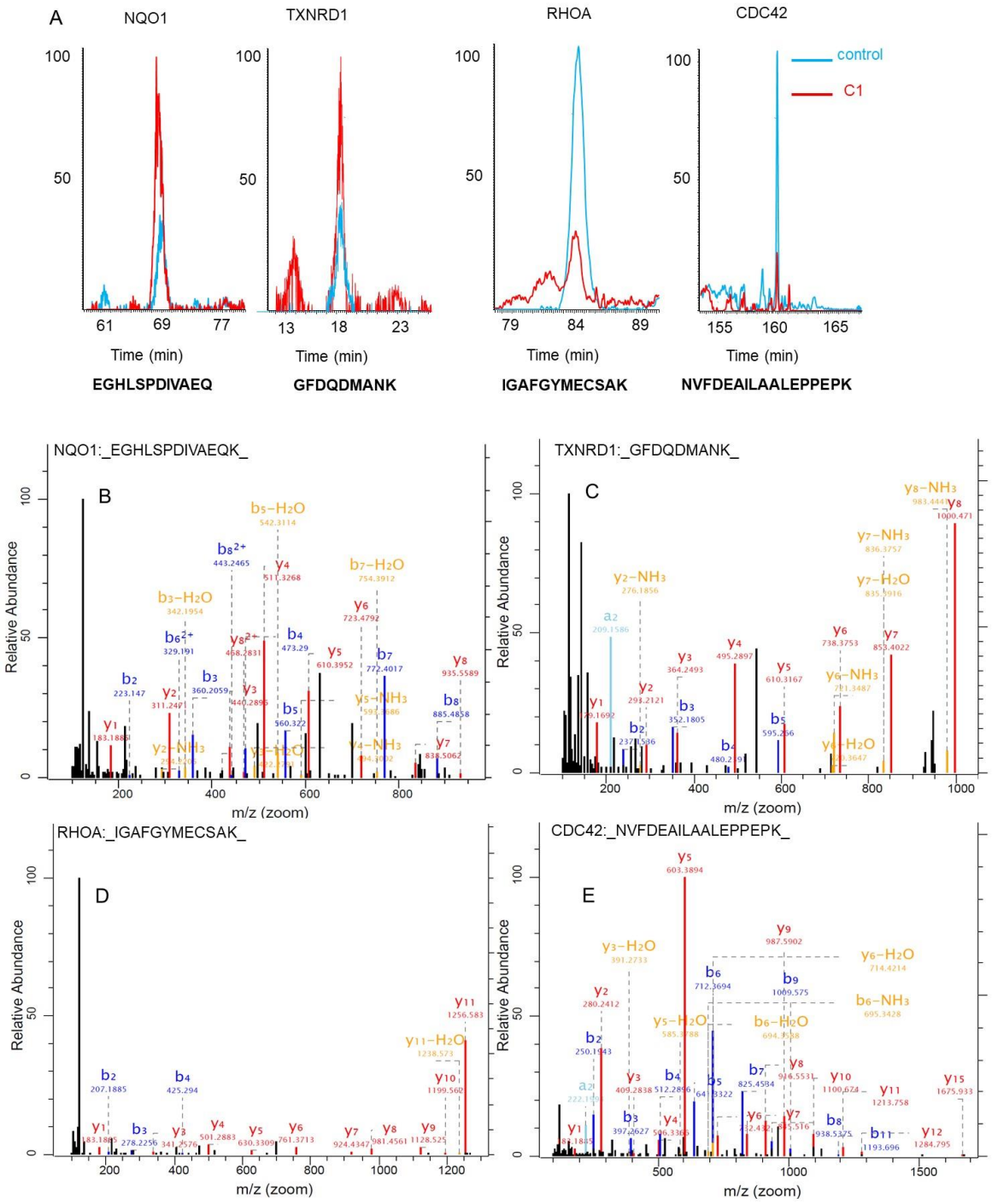

Fig. S8. (A) Chromatogram of selected peptides of four representative proteins which play vital role in Nrf2 (*NQO1* and *TXNRD1*) and *RHO* (*RHOA* and *CDC42*) pathways. Upregulations of Nrf2 pathway but downregulations of RHO pathway were observed, by comparing the peak abundances between control

and C_1 treatment. (B, C, D, E) Representative MS/MS sequence of unique peptides of *NQO1*, *TXNRD1*, *RHOA* and *CDC42*, b and y ions were annotated.

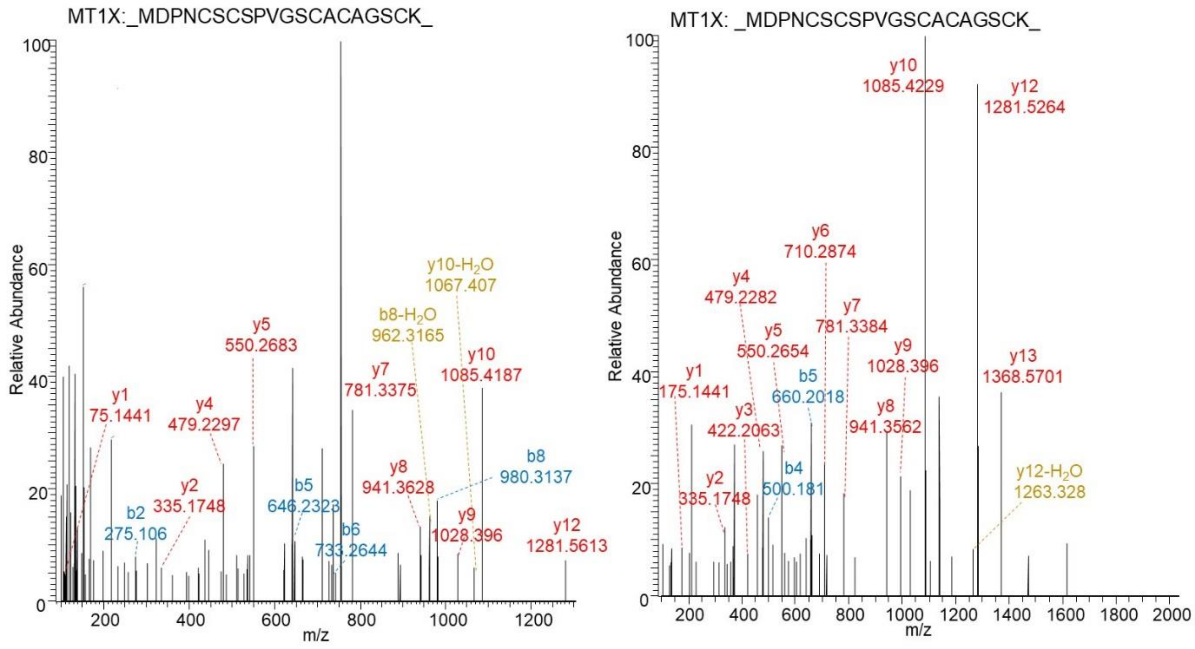

Fig. S9. Representative MS/MS sequence of unique peptides of *MT1X*, b and y ions were annotated.

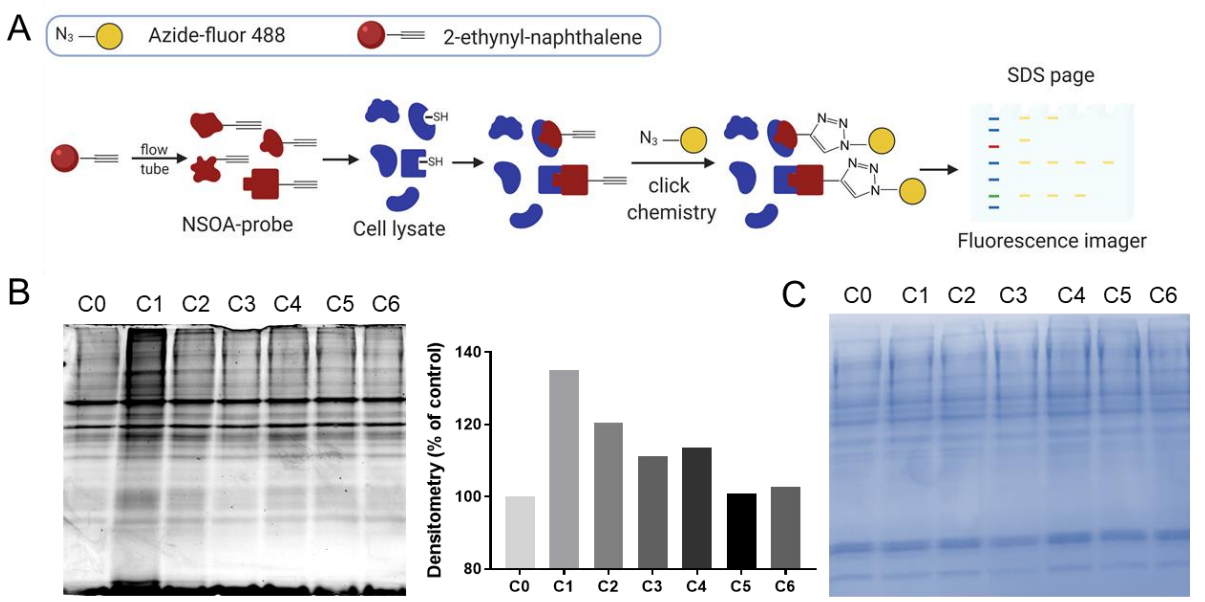

Fig. S10. (A) Workflow of ethynyl-naphthalene probe assay. 2-ethynyl-naphthalene was subjected to atmospheric oxidation to mimic NSOA. The ethynyl-NSOA products were dosed to BEAS-2B cells and proteins of targets were alkylated. Copper-catalyzed click chemistry was used to link Azide-fluor 488 to proteins which were further detected by in-gel fluorescence imaging. (B) In-gel fluorescence imaging proteins alkylated by ethynyl-NSOA. Dark protein bands indicate proteins alkylated by ethynyl-NSOA, and further linked to fluorophore. The densitometric data of western blot were quantified by ImageJ and presented by a column graph. (C) SDS-PAGE stained by Coomassie Blue R-250 was used to show the consistence of total protein concentration in different treatments.

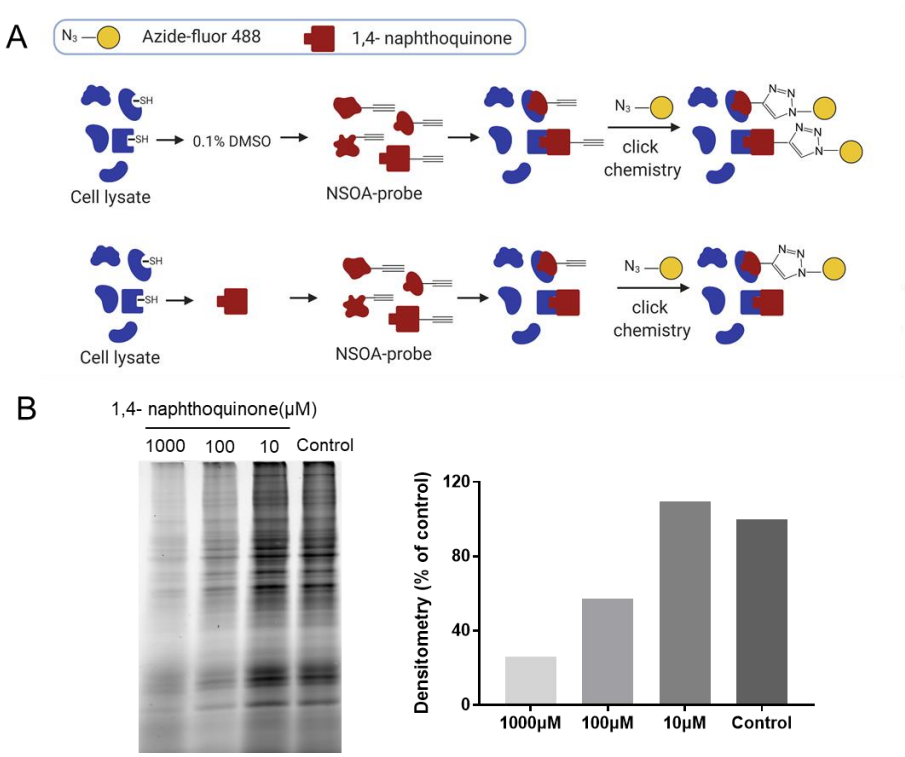

Fig. S11. (A) Workflow of competition assay of NSOA and 1,4-naphthoquinone conducted by on-gel Activity-Based Protein Profiling (ABPP) method. 10, 100, or 1000 μM of 1,4- naphthoquinone was pre-incubated with BEAS-2B cell lysate for 1h, and then 500 μM of ethynyl-NSOA from C1 treatment was added for 1h incubation. Following click chemistry, alkylated proteins were detected by in-gel fluorescence imaging. (B) In-gel fluorescence imaging proteins alkylated by ethynyl-NSOA. Dark protein bands indicate proteins alkylated by ethynyl-NSOA, and are further linked to fluorophore. The densitometric data of western blot were quantified by ImageJ and presented by a column graph. A dose-dependent competition was observed compared with control treatment without 1,4-naphthoquinone.

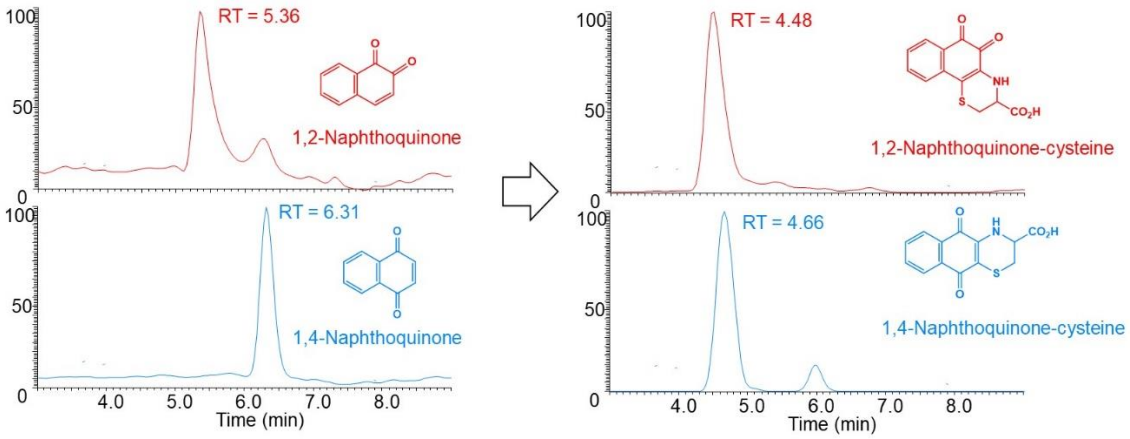

Fig. S12. Chromatograms of 1,2 – naphthoquinone (red), 1,4 – naphthoquinone (blue) and their cysteine adducts via Michael addition, by incubating 100 µM of free cysteine and 10 µM of authentic standards of naphthoquinones. Note that the retention time of 1,4 – naphthoquinone adduct is ~0.2 min later than 1,2 – naphthoquinone adduct.

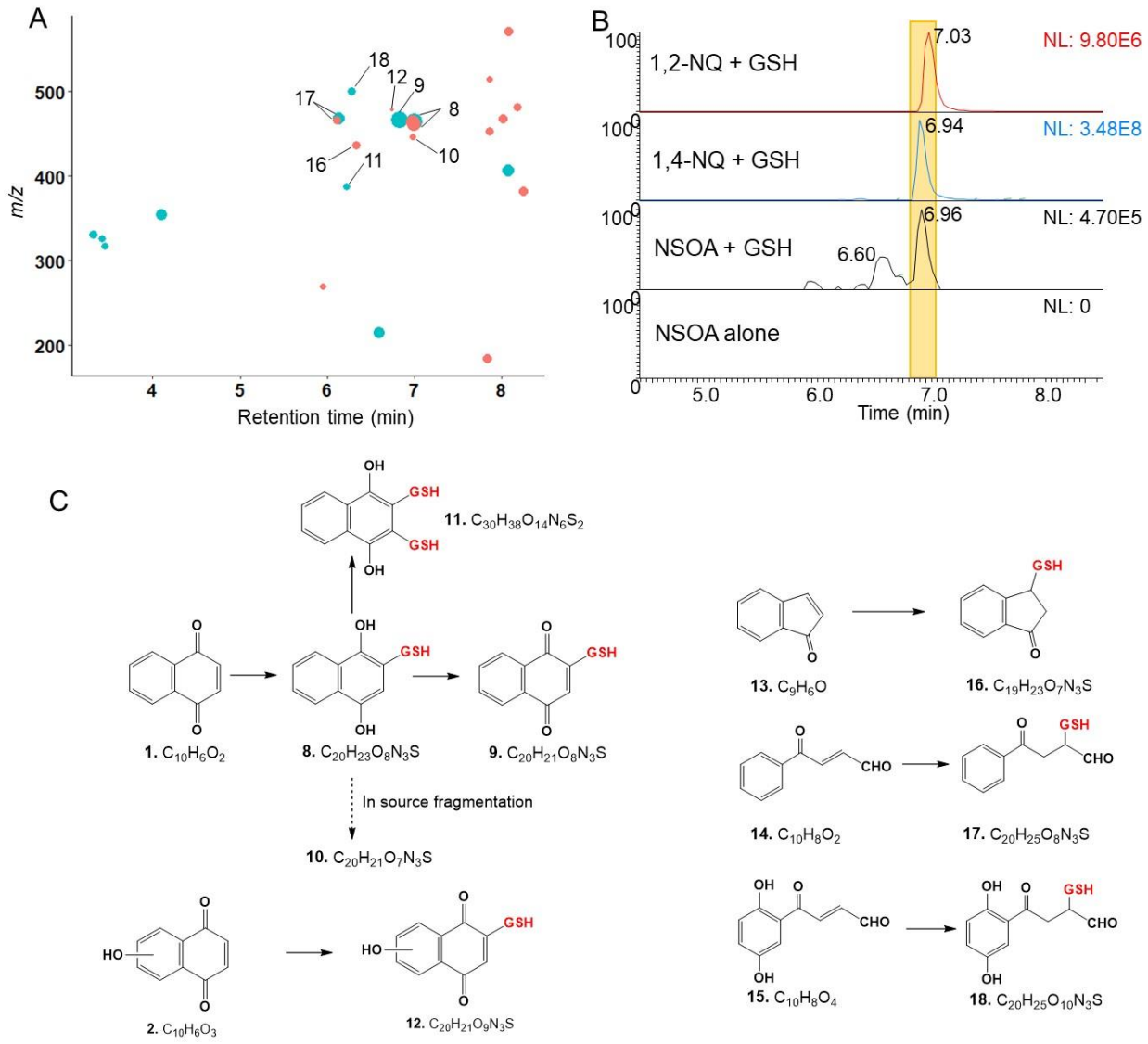

Fig. S13. Nontargeted identification of unsaturated carbonyls reactive towards reduced glutathione (GSH). (A) GSH adducts were detected after incubation. The size of each dot is proportional to the peak intensity. Red represents peaks detected under ESI^-, while blue represents peaks detected under ESI^+. The x-axis represents the retention time of GSH adducts on C18 column in UPLC. (B) Authentic standard was used to confirm chemical **8** as the GSH adducts of 1,4 – naphthoquinone (rt=6.96 min). Top two panel shows the chromatograms of GSH adducts of naphthoquinones from authentic standards (10 µM).

The third panel shows the chromatograms of GSH adducts of 1,4-naphthoquinone NSOA. (C) Proposed reaction pathways of unsaturated carbonyls **1**, **2, 13, 14,** and **15** with GSH.

SI References

1. X. Zhang, *et al.,* A novel framework for molecular characterization of atmospherically relevant organic compounds based on collision cross section and mass-to-charge ratio. *Atmos. Chem. Phys.* **16,**12945-12959 (2016).
2. C.L. Wilkins, S. Trimpin, Ion mobility spectrometry-mass spectrometry: theory and applications (CRC press) (2010).
3. G.A. Eiceman, Z. Karpas, H.H. Hill Jr, Ion mobility spectrometry (CRC press) (2013).
4. W.F. Siems, L.A. Viehland, H.H. Hill Jr, Improved momentum-transfer theory for ion mobility. 1. Derivation of the fundamental equation. *Anal. Chem*. **84**, 9782-9791 (2012).
5. E.A. Mason EA, H.W. Jr Schamp, Mobility of gaseous lons in weak electric fields. *Ann. Phys*. **4**, 233-270 (1958).
6. J.E. Krechmer *et al.,* (2016) Ion mobility spectrometry-mass spectrometry (IMS-MS) for on-and offline analysis of atmospheric gas and aerosol species. *Atmos. Meas. Tech.* **9**, 3245–3262 (2016).
7. M. Mesleh, J. Hunter, A. Shvartsburg, G.C. Schatz, M.F. Jarrold, (1996) Structural information from ion mobility measurements: effects of the long-range potential. *J. Phys. Chem.* **100**, 16082-16086 (1996).
8. A. Shvartsburg, M.F. Jarrold, An exact hard-spheres scattering model for the mobilities of polyatomic ions. *Chem. Phys. Lett.* **261**, 86-91(1996).
9. T.N. Olney, N. Cann, G. Cooper, C.E. Brion, Absolute scale determination for photoabsorption spectra and the calculation of molecular properties using dipole sum-rules. *Chem. Phys.* **223**, 59-98 (1997).
10. M.D. Hanwell *et al.,* Avogadro: an advanced semantic chemical editor, visualization, and analysis platform. *J. Cheminformatics* **4,** 17 (2012).
11. M.W. Schmidt *et al.,* General atomic and molecular electronic structure system. *J. Comput. Chem.* **14**, 1347-1363 (1993).
12. H. Kim et al., Experimental and theoretical investigation into the correlation between mass and ion mobility for choline and other ammonium cations in N_2. *Anal. Chem*. **80**, 1928-1936 (2018).
13. J.W. Lee, H.H.L. Lee, K.L. Davidson, M.F. Bush, H.I. Kim, Structural characterization of small molecular ions by ion mobility mass spectrometry in nitrogen drift gas: improving the accuracy of trajectory method calculations. *Analyst* **143**,1786-1796 (2018).
14. H. Tong *et al.,* Reactive oxygen species formed by secondary organic aerosols in water and surrogate lung fluid. *Environ. Sci. Technol.* **52**, 11642-11651 (2018).
15. R.T. Weber, Xenon Data Processing Reference (Bruker Instruments: Billerica, MA) (2012).
16. G.R. Eaton, S.S. Eaton, D.P. Barr DP, R.T. Weber RT, Quantitative EPR (Springer Science & Business Media) (2010).
17. P.J. Boersema, R. Raijmakers, S. Lemeer, S. Mohammed, A.J. Heck, Multiplex peptide stable isotope dimethyl labeling for quantitative proteomics. *Nat Protoc*. **4**, 484-494 (2009).
18. J.X. Sun et al., Identification of Chemicals that Cause Oxidative Stress in Oil Sands Process-Affected Water. *Environ. Sci. Technol.* **51**, 8773-8781(2017).
19. M.R. Dalman, A. Deeter, G. Nimishakavi, Z.H. Duan, Fold change and p-value cutoffs significantly alter microarray interpretations. *BMC bioinformatics*, **13**, (2012).